Thermal photon to dilepton ratio in high energy nuclear collisions

Jajati K. Nayak, Jane Alam, Sourav Sarkar and Bikash Sinha

Variable Energy Cyclotron Centre, 1/AF, Bidhan Nagar , Kolkata - 700064

(Dated: February 3, 2009)

The ratio of transverse momentum distribution of thermal photons to dilepton has been evaluated. It is observed that this ratio reaches a plateau beyond a certain value of transverse momentum. We argue that this ratio can be used to estimate the initial temperature of the system by selecting the transverse momentum and invariance mass windows judiciously. It is demonstrated that if the radial flow is large then the plateau disappear and hence a deviation from the plateau can be used as an indicator of large radial flow. The sensitivity of the results on various input parameters has been studied.

I. INTRODUCTION

Collisions between nuclei at ultra-relativistic energies produce charged particles - either in the hadronic or in the partonic state, depending on the collision energy. Interaction of these charged particles produce real and virtual photons (lepton pairs). Because of their nature of interaction, the mean free path of electromagnetic (EM) radiation is large compared to the size of the system formed after the collision. Therefore, EM radiation can be used as an efficient tool to understand the initial conditions of the system [1, 2, 3, 4, 5] and hence can be used to probe the quark gluon plasma (QGP) formation in heavy ion collisions (HIC). Practically, however, this is a difficult task, because on the one hand the thermal radiation from QGP has to be disentangled from those produced in initial hard collisions and from the decays of hadrons and on the other hand the evaluation of thermal photon and dilepton spectra need various inputs *such as* initial temperature (T_i), thermalization time (τ_i), equation of state (EOS), transition temperature (T_c), freeze-out temperature (T_f) etc, which are not known unambiguously. The sensitivity of the photon spectra on these inputs are demonstrated in [6, 7]. Therefore, theoretical results on transverse momentum (p_T) spectra of photons and dileptons always suffer from these uncertainties. Of course, certain constraints can be imposed on these inputs from experimental results - *e.g.* transverse mass spectra of hadrons and hadronic multiplicities are useful quantities for constraining freeze-out conditions and initial entropy production.

In the present work, therefore, we evaluate the ratio of the transverse momentum spectra of thermal photons and lepton pairs:

$$R_{em} = (d^2 N_\gamma / d^2 p_T dy)_{y=0} / (d^2 N_{\gamma^*} / d^2 p_T dy)_{y=0} \tag{1}$$

in which most of the uncertainties mentioned above are expected to get canceled so that it provides accurate information [8, 9] about the state of the matter formed initially. We calculate the ratio, R_{em} for SPS, RHIC and LHC energies.

The paper is organized as follows. In section II we discuss the invariant yield of thermal photons and lepton pairs . In section III, the space time evolution is outlined. Results are presented in section IV. Finally in section V, we summarize the work.

II. PRODUCTION OF THERMAL PHOTONS AND $e^+ e^-$ PAIRS

The rate of thermal dilepton production per unit space-time volume per unit four momentum volume is given by[1, 2, 3, 5]

$$\frac{dN}{d^4 p d^4 x} = \frac{\alpha}{12\pi^4 M^2} L(M^2) \mathrm{Im}\Pi_\mu^{\mathrm{R}\,\mu} f_{BE} \tag{2}$$

α is EM coupling, $\mathrm{Im}\Pi_\mu^\mu$ is the imaginary part of the retarded photon self energy and f_{BE} is the Bose-Einstein factor which is a function of $u^\mu p_\mu$ for a thermal system having four velocity u^μ at each space-time point of the system, $p^2 (= p_\mu p^\mu) = M^2$ is the invariant mass square of the lepton pair and

$$L(M^2) = \left(1 + \frac{2m^2}{M^2}\right) \sqrt{1 - 4\frac{m^2}{M^2}} \tag{3}$$

arises from the final state leptonic current involving Dirac spinors. m in Eq. 3 is the lepton mass.

The real photon production rate can be obtained from the dilepton emission rate by replacing the product of the EM vertex $\gamma^* \to l^+ l^-$, the term involving final state leptonic current and the square of the (virtual) photon propagator by the polarization sum ($\sum_{\mathrm{polarization}} \epsilon^\mu \epsilon^\nu = -g^{\mu\nu}$) for the real photon.

Finally the phase space factor for the lepton-pairs should be replaced by that of the photon to obtain the photon emission rate,

$$E\frac{dN}{d^4xd^3p} = \frac{g^{\mu\nu}}{(2\pi)^3}\mathrm{Im}\Pi_{\mu\nu}f_{BE} \qquad (4)$$

(see [1, 2, 3, 5] for details).

The results given above is correct up to order $e^2(\sim \alpha)$ in EM interaction but exact, in principle, to all order in strong interaction. Now it is clear form Eqs. 2 and 4 that for the evaluation of photon and dilepton production rates one needs to evaluate the imaginary part of the photon self energy. The Cutkosky rules or thermal cutting rules give a systematic procedure to express the imaginary part of the photon self energy in terms of the physical amplitude.

A. Thermal photons

Ideally, one wants to detect photons from QGP. However, the experimental measurements contain photons from various processes e.g, from the hard collisions of initial state partons of the colliding nuclei, thermal photons from quark matter and hadronic matter and photons from the hadronic decays after freeze-out. The contributions from the initial hard collisions of partons is under control via perturbative QCD (pQCD). The data from pp collisions will be very useful to validate pQCD calculations. Photons from the hadronic decays ($\pi^0 \to \gamma\gamma$, $\eta \to \gamma\gamma$ etc.) can be reconstructed, in principle, by invariant mass analysis. But the most challenging task is to separate the thermal photons originating from the hadronic phase, which needs careful theoretical estimation.

The invariant yield of thermal photons can be written as

$$\frac{d^2N_\gamma}{d^2p_Tdy} = \sum_{i=Q,M,H}\int_i \left(\frac{d^2R_\gamma}{d^2p_Tdy}\right)_i d^4x \qquad (5)$$

where $i \equiv Q, M, H$ represents QGP, mixed (coexisting phase of QGP and hadrons) and hadronic phases respectively. $(d^2R/d^2p_Tdy)_i$ is the static rate of photon production from the phase i, which is convoluted over the expansion dynamics through the integration over d^4x.

1. Thermal photons from Quark Gluon Plasma

The contribution from QGP to the spectrum of thermal photons due to annihilation ($q\bar{q}\to g\gamma$) and Compton ($q(\bar{q})g \to q(\bar{q})\gamma$) processes has been calculated in [10, 11] using hard thermal loop (HTL) approximation [12]. Later, it was shown that photons from the processes [13]: $gq\to gq\gamma$, $qq\to qq\gamma$, $qq\bar{q}\to q\gamma$ and $gq\bar{q}\to g\gamma$ contribute in the same order $O(\alpha\alpha_s)$ as Compton and annihilation processes. The complete calculation of emission rate from QGP to order α_s has been performed by resuming ladder diagrams in the effective theory [14]. In the present work this rate has been used. The temperature dependence of the strong coupling, α_s has been taken from [15].

2. Thermal photons from hadrons

For the photon spectra from hadronic phase we consider an exhaustive set of hadronic reactions and the radiative decay of higher resonance states [16, 17, 18]. The relevant reactions and decays for photon production are: (i) $\pi\pi \to \rho\gamma$, (ii) $\pi\rho \to \pi\gamma$ (with all possible mesons in the intermediate state [18]), (iii)$\pi\pi \to \eta\gamma$ and (iv) $\pi\eta \to \pi\gamma$, $\rho \to \pi\pi\gamma$ and $\omega \to \pi\gamma$. The corresponding vertices's are obtained from various phenomenological Lagrangians described in detail in Ref. [16, 17, 18]. The reactions involving strange mesons: $\pi K^* \to K\gamma$, $\pi K \to K^*\gamma$, $\rho K \to K\gamma$ and $K K^* \to \pi\gamma$ [19] have also been incorporated in the present work. Contributions from other decays, such as $K^*(892) \to K\gamma$, $\phi \to \eta\gamma$, $b_1(1235) \to \pi\gamma$, $a_2(1320) \to \pi\gamma$ and $K_1(1270) \to \pi\gamma$ have been found to be small [20] for $p_T > 1$ GeV. All the isospin combinations for the above reactions and decays have properly been taken into account. The effects of hadronic form factors [19] have also been incorporated in the present calculation.

B. Thermal dileptons

Like photons, dileptons can also be used as an efficient probe for QGP diagnostics, provided one can subtract out contributions from Drell-Yan process, decays of vector mesons within the life time of the fire ball and hadronic decays occurring after the freeze-out. Like hard photons, lepton pairs from Drell-Yan processes can be estimated by pQCD. The p_T spectra of thermal lepton pair suffer from the problem of indistinguishability between QGP and hadronic sources unlike the usual invariant mass (M) spectra which shows characteristic resonance peaks in the low M region. The invariant transverse momentum distribution of thermal dileptons (e^+e^- or

virtual photons, γ^*) is given by:

$$\frac{d^2N_{\gamma^*}}{d^2p_Tdy} = \sum_{i=Q,M,H} \int_i \left(\frac{d^2R_{\gamma^*}}{d^2p_TdydM^2}\right)_i dM^2d^4x.$$

(6)

The limits for integration over M can be fixed judiciously to detect contributions from either quark matter or hadronic matter (see Fig.1). Experimental measurements [21, 22] are available for different M window.

1. Dileptons from QGP

In the plasma phase the lowest order process producing lepton pair is $q\bar{q} \rightarrow \gamma^* \rightarrow l^+l^-$. QCD corrections to this rate have been obtained for a QCD plasma at finite temperature in Refs. [23, 24] up to order $O(\alpha^2\alpha_s)$. In the present work contribution up to $O(\alpha^2\alpha_s)$ has been considered.

2. Dileptons from Hadrons

The following parametrization [5, 25] has been used to evaluate the dilepton emission rates from light vector mesons (ρ, ω and ϕ):

$$\begin{aligned}\frac{d^2R_{\gamma^*}}{dM^2d^2p_Tdy} &= \frac{\alpha^2}{2\pi^3}f_{BE}[\frac{f_V^2M\Gamma_V}{(M^2-m_V^2)^2+(M\Gamma_V)^2} \\ &+\frac{1}{8\pi}\frac{1}{1+exp((w_0-M)/\delta)} \\ &\times(1+\frac{\alpha_s}{\pi})].\end{aligned}$$

(7)

These parameterizations are consistent with the experimental data from $e^+e^- \rightarrow V(\rho,\omega$ or $\phi)$ processes [5, 25, 26]. Here, f_{BE}, is the Bose-Einstein distribution. f_V is the coupling between the EM current and vector meson fields, m_V and Γ_V are the masses and widths of the vector mesons and ω_0 is the continuum threshold above which the asymptotic freedom is restored. We have taken $\alpha_s = 0.3$, $\delta = 0.2 GeV$, $\omega_0 = 1.3$ GeV for ρ and ω. For ϕ we have taken $\omega_0 = 1.5$ GeV and $\delta = 1.5$ GeV. The EM current in terms of ρ, ω and ϕ field can be expressed as $J_\mu = J_\mu^\rho + J_\mu^\omega/3 - J_\mu^\phi/3$. Therefore, the contributions from ω and ϕ will be down by a factor of 9.

III. SPACE-TIME EVOLUTION

The matter formed after ultra-relativistic heavy ion collisions undergo space-time evolution, which can be described by relativistic hydrodynamics. In the present work the space time evolution of the system has been studied using ideal relativistic hydrodynamics in (2+1) dimension [27] with longitudinal boost invariance [28] and cylindrical symmetry. The initial temperature(T_i) and thermalization time (τ_i) are constrained by the following equation [29] for an isentropic expansion:

$$T_i^3\tau_i \approx \frac{2\pi^4}{45\xi(3)}\frac{1}{4a_{eff}}\frac{1}{\pi R_A^2}\frac{dN}{dy}.$$

(8)

where, $dN/dy=$ hadron multiplicity, R_A is the radius of the system, $\xi(3)$ is the Riemann zeta function and $a = \pi^2g/90$ ($g = 2 \times 8 + 7 \times 2 \times 2 \times 3 \times N_F/8$) is the degeneracy of the massless quarks and gluons in the QGP, $N_F=$number of flavours. The values of initial temperatures and thermalization times for various beam energies are shown in table I. The initial energy density,$\epsilon(\tau_i, r)$ and radial velocity, $v_r(\tau_i, r)$ profiles are taken as:

$$\epsilon(\tau_i, r) = \frac{\epsilon_0}{1 + e^{\frac{r-R_A}{\delta}}}$$

(9)

and

$$v_r(\tau_i, r) = v_0 \left(1 - \frac{1}{1 + e^{\frac{r-R_A}{\delta}}}\right),$$

(10)

where the surface thickness, $\delta = 0.5$ fm. We have taken $v_0 = 0$, which can reproduce the measured hadronic spectra at SPS and RHIC energies [6, 30]. So far there is no consensus on the value of T_c, it varies from 151 MeV [31] to 192 MeV [32]. In the present work we assume $T_c = 192$ MeV. In a first order phase transition scenario - we use the bag model EOS for the QGP phase and for the hadronic phase all the resonances with mass ≤ 2.5 GeV have been considered [33].

To show the sensitivity of the results on the EOS we also use the lattice QCD EOS for $T \geq T_c$ [34]. For the hadronic matter (below T_c) all the resonances with mass ≤ 2.5 GeV have been considered [33]. For the transition region the following parametrization has been used [35].

$$s = f(T)s_q + (1 - f(T))s_h$$

(11)

where s_q (s_h) is the entropy density of the quark (hadronic) phase at T_c and

$$f(T) = \frac{1}{2}(1 + tanh(\frac{T - T_c}{\Gamma}))$$

(12)

the value of the parameter Γ can be varied to make the transition strong or weak first order. Results for various values of Γ are given below.

TABLE I: The values of various parameters - thermalization time (τ_i), initial temperature (T_i), freeze-out temperature (T_f) and hadronic multiplicity dN/dy - used in the present calculations.

Accelerator	$\frac{dN}{dy}$	$\tau_i(fm)$	T_i(GeV)	T_f (MeV)
SPS	700	1	0.2	120
RHIC	1100	0.2	0.4	120
LHC	2100	0.08	0.7	120
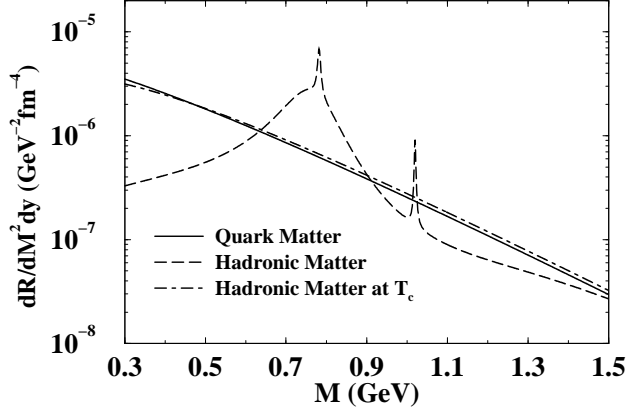
FIG. 1: The invariant mass distributions of thermal dileptons from QGP and hadronic matter at $T = 200$ MeV. Solid (dashed) line indicates the emission rates from QGP (hadronic matter). The dot-dashed line stands for emission rate from hadronic matter at the transition temperature (see text).

IV. RESULTS

The values of the initial and freeze-out parameters shown in table I along with the EOS mentioned above have been used as inputs to hydrodynamic calculations. The experimental data from SPS on hadrons [36], photons [37] and M distribution of dileptons [38] have been reproduced in [30], [39, 40] and [41] respectively by using these inputs. The values of the initial parameters for SPS agree with the results obtained from the analysis of photon spectra in Refs. [42, 43, 44, 45]. Recently the data from PHENIX collaboration at RHIC [46, 47] has also been explained in [6] (see also [48]) with the parameters mentioned in table I. The lepton pairs measured by NA60 collaboration [49, 50] in In-In collisions has been explained by spectral broadening of ρ [51, 52].

The emission rate from hadronic and quark matter at a temperature of 200 MeV has been displayed in Fig. 1. The contribution from QGP dominates over its hadronic counterpart (without any medium effects) for $M < 600$ MeV and $M > 1.1$ GeV, therefore, these windows are better suited for the detection of QGP. However, it should be men-
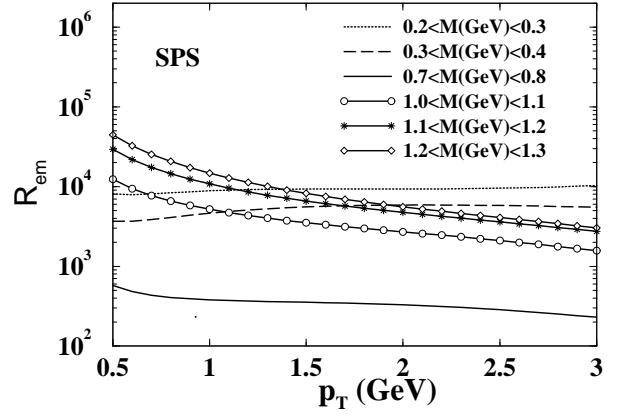

FIG. 2: The thermal photon to dilepton ratio, R_{em} as a function of transverse momentum, p_T for various invariant mass window.
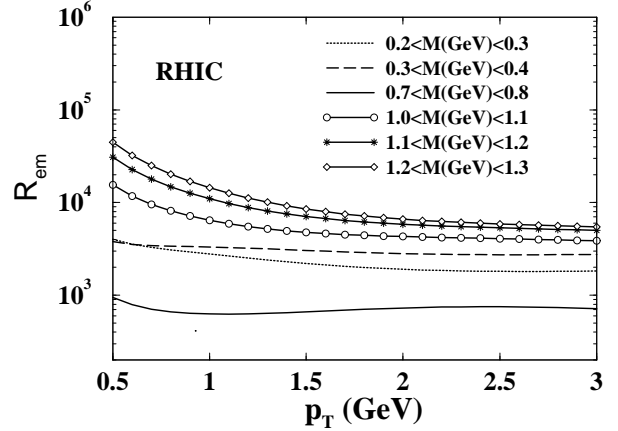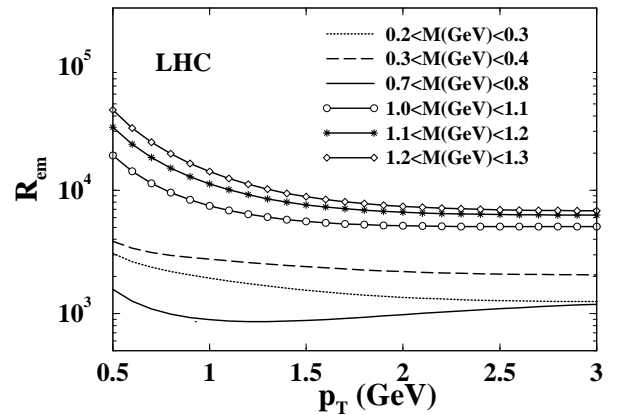

FIG. 3: Same as Fig. 1 for RHIC energy
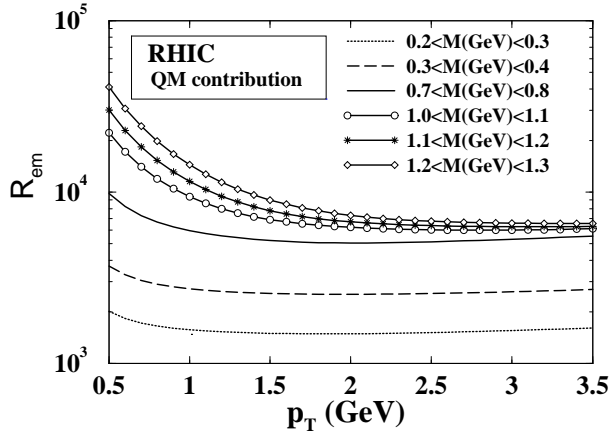

FIG. 4: Same as Fig. 1 for LHC energy
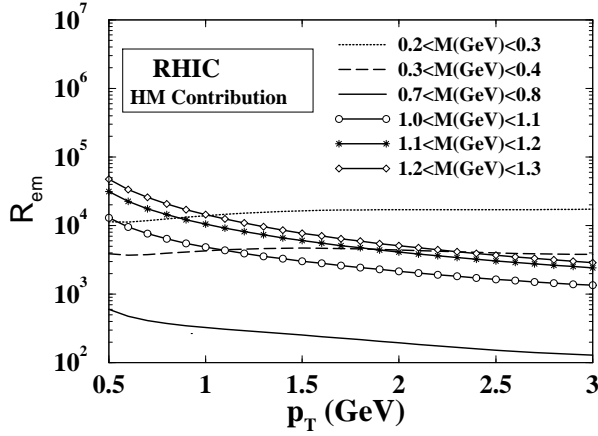
FIG. 5: Same as Fig. 2 for quark matter phase only.

FIG. 6: Same as Fig. 2 for hadronic phase only.

FIG. 7: The variation R_{em} with p_T for invariant mass window, $M = 0.7 - 0.8$ GeV. An unrealistically large value to radial flow has been given initially to demonstrate that large flow can destroy the plateau structure of R_{em}. Other inputs are similar to those of Figs.3 and 4.

FIG. 8: R_{em} as a function of p_T for different values of T_c for invariant mass windows, $M = 0.7 - 0.8$ GeV and $M = 1.2 - 1.3$ GeV.

tioned here that the modification of the spectral functions of vector mesons (especially ρ and ω) - pole shift [53] or broadening [26] may give rise to dileptons at the lower M region making it difficult to detect contributions from QGP. The change in the hadronic spectral function will enhance the dileptons from the hadronic contribution in the lower mass ($M < 600 MeV$) window, however the overall structure in the ratio, R_{em} will not change appreciably. At the transition temperature (~ 200 MeV) if one assumes the vector mesons masses go zero *a la* Brown-Rho scaling [53] then all the peaks in the dilepton spectra disappeared and the rates obtained from EM current-current correlator (dot-dashed line) are close to the rate from QGP, indicating that the $q\bar{q}$ interaction in the vector channel has become very weak, signaling the onset of deconfinement. This also indicates the quark-hadron duality [54, 55] near the transition point.
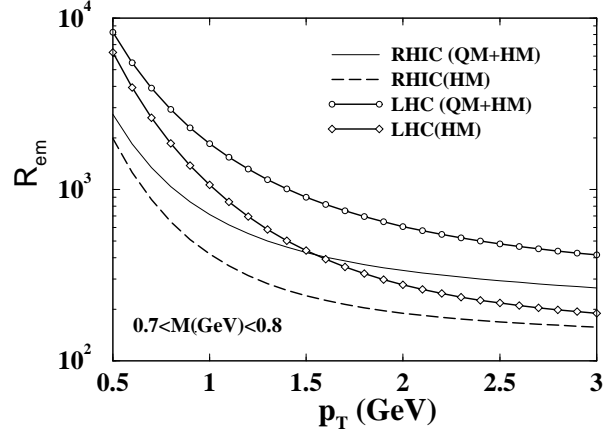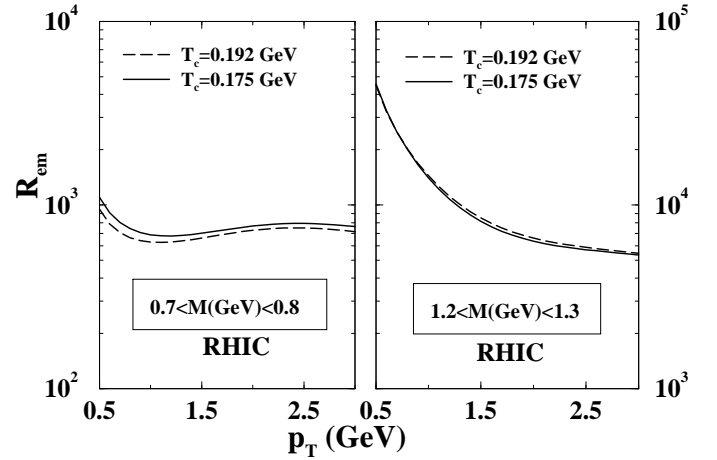
It is well known that the p_T spectra of photons and lepton pairs are sensitive to the values of initial temperature T_i, v_0, T_f and EOS. The T_c dependence of the p_T distribution is found to be negligibly small [6]. As we have mentioned before though these parameters can be constrained from the measured multiplicity and freeze-out spectra there remains still some room to vary these quantities in order to be able to describe the experimental data.

The p_T dependence of the ratio, R_{em} for SPS, RHIC and LHC energies are shown in Figs. 2, 3 and 4 respectively. It is observed that at a given p_T, the
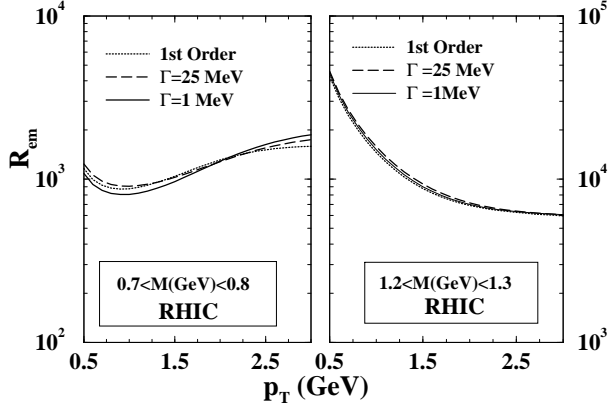
FIG. 9: R_{em} as a function of p_T for different EOS for invariant mass windows, $M = 0.7 - 0.8$ GeV and $M = 1.2 - 1.3$ GeV.
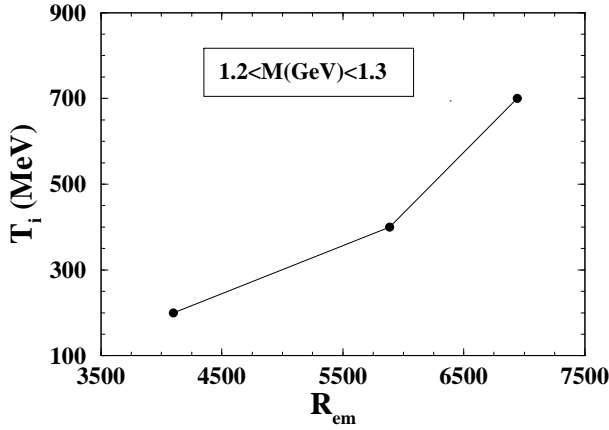

FIG. 10: Initial temperature is plotted as function $R_{em}(p_T = 2.5 \text{GeV})$ for the M window, $M = 1.2 - 1.3$ GeV.

ratio decreases with M, reaches a minimum around ρ-peak and increases beyond the ρ-peak. This trend is valid for all the cases, *i.e.* SPS, RHIC and LHC as expected because at a given p_T the R_{em} is actually the inverse of the invariant mass distribution of lepton pairs (the denominator *i.e.* the photon spectra is same for all the mass windows). It is observed from Figs. 2, 3 and 4 that the ratio, R_{em} decreases with T_i for given p_T for M below the ρ-peak and the opposite behaviour is observed above the ρ-peak. The slope of the ratio at low p_T also indicates substantial change with increasing M, the slope is minimum at the ρ-peak. Therefore, the minimum of the slope may be used to locate the effective mass of the vector meson in medium.

It is clear from the results displayed in Figs. 2 3 and 4 that the quantity, R_{em}, reaches a plateau beyond $p_T = 1.5$ GeV for all the three cases *i.e.* for SPS, RHIC and LHC. It may be noted here that the degree of flatness increases from SPS to RHIC and LHC. As mentioned before for all the three cases, except T_i all other quantities *e.g.* T_c, v_0 and EOS are same, so the difference in the value of R_{em} in the plateau region originates due to different values of initial temperature, indicating this can be a measure of T_i.

The following analysis will be useful to understand the origin of the plateau at high p_T region. The strong three momentum dependence in the dilepton and photon emission rates (Eqs. 2 and 4 respectively) originates from the thermal factor, $f_{BE}(E, T)$. For a static system the energy, E can be written as $E = M_T coshy$, where $M_T = \sqrt{p_T^2 + M^2}$ $y = tanh^{-1}p_z/E$. At high $p_T(>> M)$, $M_T \approx p_T$, the exponential momentum dependence become same for real photon ($M^2 = 0$) and dilepton ($M^2 \neq 0$) spectra and hence plateau is expected in the static ratio for large p_T for all the M values.

We recall that for an expanding system out of the two kinematic variables describing the dilepton spectra, p_T is affected by expansion but M remains unchanged. The range of M under present study is $0.3 < M(\text{GeV}) < 1.3$. The energy, E appearing in both the photon and dilepton emission rates should be replaced by $u^\mu p_\mu$ for a system expanding with space-time dependent four velocity u^μ. Under the assumption of cylindrical symmetry and longitudinal boost invariance u^μ can be written as

$$u^\mu = \gamma_r(t/\tau, v_r cos\phi, v_r sin\phi, z/\tau) \qquad (13)$$

where $\tau = \sqrt{t^2 - z^2}$ $t = \tau cosh\eta$, $z = \tau sinh\eta$, $v_r(\tau, r)$ is the radial velocity, $\gamma_r(\tau, r) = (1 - v_r(\tau, r))^{-1/2}$. The four momentum, $p^\mu = (M_T coshy, p_T, 0, M_T sinhy)$ where $p_L = m_T sinhy$. Therefore, for dilepton

$$u^\mu p_\mu = \gamma_r(M_T cosh(y - \eta) - v_r p_T cos\phi) \qquad (14)$$

for photon the factor $u^\mu p_\mu$ can be obtained by replacing M_T in Eq. 14 by p_T. The p_T dependence of the photon and dilepton spectra originating from an expanding system is predominantly determined by the thermal factor f_{BE}. Therefore, we discuss following three scenarios. (i)At high $p_T(>> M)$, $M_T \approx p_T$, the exponential momentum dependence become same for real photon and dilepton spectra, hence for large p_T a plateau is obtained in the ratio, R_{em} (Figs 2-4). In other words, the effect of radial flow on the photon and dilepton is similar at high p_T region. (ii)If the large M pairs originate from early time (when the flow is small) the ratio, R_{em} which includes space-time dynamics will be close to the

static case and hence will show plateau. (iii) However, at late time when the radial flow is large and M is comparable to or larger than p_T the effect of flow on dilepton will be larger (receives larger radial kick due to non-zero M) than the photon and hence the plateau may disappear. Therefore, the disappearance of plateau structure in R_{em} in moderate or high M region will indicate the presence large radial flow. This can be understood from the results shown in Figs 5 and 6.

In Fig. 5 the ratio has been displayed only for quark matter. Here the flow is expected to be lower within the present framework of present study. A plateau is observed for all the M windows. It is observed that for high M (~ 1.2 GeV) and low M (~ 0.3 GeV) the ratio for QM is close to the total for LHC energy (not shown separately).

In Fig.6 the ratios has been displayed for hadronic matter only. Here the flow is expected to be very large. Within the ambit of the present modeling the contribution from the hadronic matter is overwhelmingly large in the M region, $0.7 < M < 0.8$ GeV. Therefore, this region will have large effects from the radial flow and hence it may destroy the plateau. This is clearly seen in Fig. 6 for the curve corresponding to $0.7 < M < 0.8$ GeV.

To demonstrate the effect of flow on the plateau we use an initial velocity profile (which gives rise to stronger radial flow than Eq. 10) of the form $v_r(\tau_i, r) = v'_0 \frac{r}{R_A}$ with an *unrealistically* large value of $v'_0 \sim 0.5$. These inputs are used only for results shown in Fig.7, which clearly indicates the disappearance of plateau. Variation of R_{em} with p_T corresponding to hadronic phase is steeper than the total because of larger radial flow in the late stage of the evolution.

Now we demonstrate the effect of other parameters on R_{em}. The value of T_c has large uncertainties. Therefore, we show the sensitivity of the results on T_c in Fig. 8 for two invariant mass windows. The results are insensitive to T_c.

The effect of the EOS on R_{em} is demonstrated in Fig. 9, by varying Γ in Eq. 12. It is observed that the effect of EOS on R_{em} for both the mass windows are small. Similar to the effect of T_c, the larger mass window ($1.2 \leq M(\text{GeV}) < 1.3$) is less affected by the change in EOS. This is because the effect radial flow (and other hydrodynamic effects) are less at early times from where higher mass lepton pairs originate. Replacement of lattice QCD EOS for QGP phase by bag model shows negligible effects on R_{em}.

In Fig. 10 the dependence of $R_{em}(p_T = 2.5\text{GeV})$ is depicted as a function of T_i for $1.2 \leq M(\text{GeV}) < 1.3$. This mass window is selected because the contributions from the hot quark matter phase dominates this region and the effects of T_c, EOS etc are least here. $p_T = 2.5$ GeV is taken because R_{em} achieved
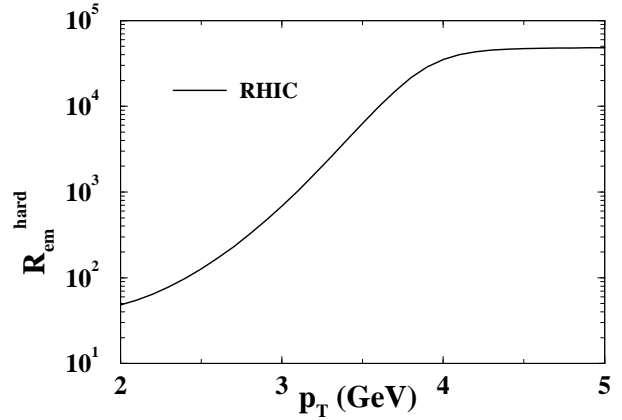

FIG. 11: The variation R_{em} for hard photons to dileptons ratio as a function of p_T for $\sqrt{s_{NN}} = 200$ GeV and invariant mass window, $M = 0.2 - 0.3$ GeV.

a complete plateau at this value of transverse momentum. The change in R_{em} from SPS to RHIC is about 40% and from RHIC to LHC this is about 20%. A simultaneous measurements of photons and dileptons with required accuracy, will be useful to disentangle the effects of flow and true average temperature in a space-time evolving system formed in heavy ion collisions at ultra-relativistic energies.

We have evaluated R_{em}^{pQCD}, the ratio $(d^2 N_\gamma / d^2 p_T dy)_{y=0}/(d^2 N_{\gamma^*}/d^2 p_T dy)_{y=0}$ for hard processes using pQCD (Fig. 11). The hard photon contributions has been constrained to reproduce the PHENIX data [56] for pp collisions at $\sqrt{s_{NN}} = 200$ GeV. We consider $q\bar{q} \rightarrow \gamma^* \rightarrow l^+ l^-$, $q\bar{q} \rightarrow g\gamma^*$ and $qg(\bar{q}) \rightarrow q\bar{q}\gamma^*$ for the lepton pair production. The M integration of lepton pair spectra (Eq. 6) is done over the range $0.2 \leq M(\text{GeV}) \leq 0.3$. We observe that R_{em}^{pQCD} increases for p_T up to ~ 3 GeV, above which it reaches a plateau. Therefore, for $p_T \sim 1-3$ GeV, R_{em} for the thermal and pQCD processes show different kind of behaviour. The plateau arises from the fact that at large p_T both photon and dilepton show power law behaviour [57, 58]. In the low p_T domain lepton pairs (photon) from pQCD processes indicate a Gaussian type [57] (power law) variation resulting in the increase of R_{em} with p_T.

V. SUMMARY AND CONCLUSIONS

We have studied the variation of R_{em}, the ratio of the transverse momentum spectra of photons and dileptons and argued that measurement of this quantity will be very useful to determine the value of the initial temperature of the system formed after heavy ion collisions. We have observed that R_{em} reaches a plateau beyond $p_T = 1.5$ GeV. The value of R_{em} in

the plateau region depends on T_i. However, the effects of flow, EOS and the dependence on the values of T_c, v_0 and other model dependences get canceled away in the ratio, R_{em}. For M above and below the ρ peak and $p_T \geq 2$ GeV the contributions from quark matter dominates, therefore these regions could be chosen to estimate the initial temperature of the system formed after the collisions.

It is well known that T_{eff}, the inverse slope (see *e.g.* [50]) extracted from the p_T spectra of EM radiation contains the effect of temperature as well as flow. We have seen that when the flow is less (in the initial stage of the evolution) the ratio, R_{em} shows a plateau for large $p_T(>> M)$, the height of the plateau in this region will give a good measure of the average temperature. However, a large flow can destroy the plateau and hence the deviation from the flatness of the R_{em} versus p_T curve may be used as a measure of flow. So a careful selection of M and p_T regions will be very helpful to disentangle the effect of true average temperature and the flow (see also [59]). In [59] it was shown that the effects of flow on high $M(> 1.5$ GeV$)$ could be quite large and in such cases the plateau in R_{em} may disappear. However, in the present work we confine in the range $0.3 < M)$GeV$) < 1.2$.

EM radiations originating from the interactions between thermal and non-thermal (high energy) partons [60, 61, 62] has been neglected in the present work. It is expected that the EM radiation from these processes and also from the pre-equilibrium stage will not affect R_{em}.

We have studied the effects of chemical off-equilibrium of mesons on the photon and dilepton production rates. This is implemented by appropriately introducing non-zero pionic chemical potential, μ_π ($\mu_\rho = 2\mu_\pi, \mu_\omega = 3\mu_\pi$) in the thermal factors [63] appearing both in photon and dilepton emission rates. We observed that the plateau structures in R_{em} do not change for RHIC and LHC, but for SPS it has little effect.

The change in hadronic spectral function at non-zero temperature and density is a field of high contemporary research interest as this is connected with the restoration of chiral symmetry in QCD. From the QGP diagnostics point of view the background contributions (photons and dileptons from thermalized hadrons) are affected due to medium effects on hadrons. Therefore, some comments on this issue are in order here.

We have checked that the p_T spectra of both photons and dileptons are sensitive to the pole shift of hadronic spectral function, as the reduction of hadronic masses [53] in a thermal bath increases their abundances and hence the rate of emission gets enhanced [5, 16, 17, 39, 40]. The invariant mass distribution of lepton pairs are sensitive to both the pole shift and broadening [26, 40, 41, 64, 65]. But the p_T spectra of the EM radiation is insensitive to the broadening of the spectral function provided the integration over the M is performed over the entire region. This is because broadening does not change the density of vector mesons significantly (see also [40]). However, the number density of vector mesons depends on the nature (shape) of the spectral function within the integration limit. Therefore, the p_T spectra may change due to broadening when the integration over M is done in a limited M domain. We have checked that doubling the ρ width ($\sim 2 \times 150$ MeV) changes R_{em} by 10%. It is important to note that the change in mass and widths can not be arbitrary it should obey certain constraints as discussed in [66]. Therefore, simultaneous measurements of p_T spectra and invariant mass distribution of real and virtual photons could be very useful to understand the nature of medium effects on hadrons [40].

[1] L. D. McLerran and T. Toimela, Phys. Rev. D **31**, 545 (1985).

[2] C. Gale and J.I. Kapusta, Nucl. Phys. B **357**, 65 (1991).

[3] H.A. Weldon, Phys. Rev. D **42**, 2384 (1990).

[4] J. Alam, S. Raha and B. Sinha, Phys. Rep. **273**, 243 (1996).

[5] J. Alam, S. Sarkar, P. Roy, T. Hatsuda and B. Sinha, Ann. Phys. **286**, 159 (2000).

[6] J. Alam, J. K Nayak, P. Roy, A. K. Dutt-Mazumder and B. Sinha, J. Phys. G **34** 871 (2007).

[7] J. Alam, D. K. Srivastava, B. Sinha and D. N. Basu, Phys. Rev. D **48** 1117 (1993).

[8] B. Sinha, Phys. Lett. B **128**, 91 (1983).

[9] S. Raha and B. Sinha, Phys. Rev. Lett. **58** 101 (1987).

[10] J. Kapusta, P. Lichard, and D. Seibert, Phys. Rev. D **44**,2774 (1991).

[11] R. Bair, H. Nakkagawa, A. Niegawa, and K. Redlich, Z. Phys. C **53**, 433(1992).

[12] E. Braaten and R. D. Pisarski, Nucl. Phys. B **337**, 569 (1990); ibid **339**, 310 (1990).

[13] P. Aurenche, F. Gelis, R. Kobes, and H. Zaraket, Phys. Rev. D **58**, 085003 (1998).

[14] P. Arnold, G. D. Moore, and L.G. Yaffe, J. High Energy Phys. **0111**, 057 (2001) ; P. Arnold, G.D. Moore, and L.G. Yaffe, J. High Energy Phys. **0112**, 009 (2001) ; P. Arnold, G.D. Moore, and L.G. Yaffe,

J. High Energy Phys. **0206**, 030 (2002).

[15] O. Kaczmarek and F. Zantow Phys. Rev D **71** 114510 (2005).

[16] S. Sarkar, J. Alam, P. Roy, A. K. Dutt-Mazumder, B. Dutta-Roy and B. Sinha, Nucl. Phys. A **634** 206 (1998).

[17] P. Roy, S. Sarkar, J. Alam and B. Sinha Nucl. Phys. A **653** 277 (1999).

[18] J. Alam, P. Roy and S. Sarkar Phys. Rev. C **71** 059802 (2005).

[19] S. Turbide, R. Rapp and C. Gale, Phys. ReV. C **69**, 014903(2004).

[20] K. L. Haglin, J. Phys. G **30** L27 (2004).

[21] S. Damjanovic for the NA60 collaboration, Nucl. Phys. A **783** 327 (2007).

[22] A. Toia, arXiv:0805.0153 [nucl-ex]

[23] T. Altherr and P. V. Ruuskanen, Nucl. Phys. B **380**, 377 (1992).

[24] M. H. Thoma and C. T. Traxler, Phys. ReV. D **56**, 198(1997).

[25] E. V. Shuryak, Rev. Mod. Phys. **65** 1 (1993).

[26] R. Rapp and J. Wambach, Adv. Nucl. Phys. **25**, 1 (2000)

[27] H. von Gersdorff, M. Kataja, L. D. McLerran and P. V. Ruskanen, Phys. Rev. D **34** 794(1986).

[28] J. D. Bjorken, Phys. Rev. D **27**, 140 (1983).

[29] R. C. Hwa and K. Kajantie, Phys. Rev. D **32**,1109 (1985).

[30] B. K. Patra, J. Alam, P. Roy, S. Sarkar and B. Sinha, Nucl. Phys. A **709** 440 (2002).

[31] Y. Aoki, Z. Fodor, S. D. Katz and K. K. Szab, Phys. Lett. B **643** 46 (2006).

[32] M. Cheng et al., Phys. Rev. D **74**, 054507 (2006).

[33] B. Mohanty and J. Alam Phys. Rev. C **68** 064903 (2003).

[34] C. Bernard et al, Phys. Rev. D **75**, 094505 (2007).

[35] M. Asakawa and T. Hatsuda Phys. Rev. D **55** 4488 (1997).

[36] H. Appelshauser et al (for NA49 Collaboration), Phys. Rev. Lett. **82** 2471 (1999).

[37] M. M. Aggarwal et al (for WA98 Collaboration), Phys. Rev. Lett. **85** 3595 (2000).

[38] G. Agakichiev for CERES collaboration, Phys. Lett. B **422** 405 (1998).

[39] J. Alam, S. Sarkar, T. Hatsuda, T. K. Nayak and B. Sinha, Phys. Rev. C **63** 021901 (R) (2001).

[40] J. Alam, P. Roy, S. Sarkar and B. Sinha, Phys. Rev. C **67** 054901 (2003).

[41] S. Sarkar, J. Alam and T. Hatsuda, J. Phys. G **30** 607 (2004).

[42] F. D. Steffen and M. H. Thoma, Phys. Lett. B **510** 98 (2001).

[43] P. Huovinen, P. V. Ruuskanen and S. S. Rasanen Phys. Lett. B **535** 109 (2002).

[44] K. Gallmeister and B. Kampfer, Phys. Rev. C **62** 057901 (2000).

[45] D. Peressounko and Yu E. Pokrovsky, hep-ph/0009025.

[46] S. S. Adler et al (for PHENIX collaboration), Phys. Rev. C **69** 034909 (2004).

[47] H. Buesching (for PHENIX collaboration), Nucl. Phys. A **774** 103 (2006).

[48] D. d'Enterria and D. Peressounko, Eur. Phys. J. C **46** 451 (2006).

[49] A. Arnaldi (for NA60 collaboration), Phys. Rev. Lett. **96** 162302 (2005).

[50] A. Arnaldi (for NA60 collaboration), **100** 022302 (2008).

[51] H. van Hees and R. Rapp, Phys. Rev. Lett. **97** 102301 (2006).

[52] J. Ruppert, C. Gale, T. Renk, P. Lichard and J. I. Kapusta, Phys. Rev. Lett. **100** 162301 (2008).

[53] G. E. Brown and M. Rho, Phys. Rev. Lett. **66** 2720 (1991).

[54] E. V. Shuryak, Nucl. Phys. A **661** 119 (1999).

[55] R. Rapp, Nucl. Phys. A **661** 33 (1999).

[56] S. Adler, (for PHENIX collaboration), Phys. Rev. D **71** 071102 (2005).

[57] R. K. Ellis, W. J. Stirling and B. R. Webber, QCD and Collider Physics, Cambridge University Press, 1996.

[58] R. D. Field, Application of Perturbative QCD, Addison-Wesley Pub. Co. 1989.

[59] T. Renk and J. Ruppert, Phys. Rev. C **77** 024907 (2008).

[60] P. Roy, J. Alam, S. Sarkar, B. Sinha and S. Raha, Nucl. Phys. **624** 687 (1997).

[61] R. J. Fries, B. Muller and D. K. Srivastava, Phys. Rev. Lett. **90** 132301 (2003).

[62] L. Bhattacharya, P. Roy, arXiv:0806.4033 [hep-ph]

[63] H. van Hees and R. Rapp, Nucl. Phys. A **806** 339 (2008).

[64] G. Q. Li, C. M. Ko and G. E. Brown *Nucl. Phys.* A **606** 568 (1996).

[65] R. Rapp, G. Chanfray and J. Wambach, Nucl. Phys. A **617** 472 (1997).

[66] S. Leupold, W. Peters and U. Mosel, Nucl. Phys. A **628** 311 (1998).